Impact of the motor magnetic model on direct flux vector control of interior PM motors

Impact of the Motor Magnetic Model on Direct Flux Vector Control of Interior PM Motors

Gianmario Pellegrino, Radu Bojoi, Paolo Guglielmi
Politecnico di Torino, Italy
(gianmario.pellegrino,radu.bojoi,paolo.guglielmi)@polito.it

***Abstract* – The stator-field-oriented, direct-flux vector control has been proven to be effective in terms of linear torque control and model independent performance at limited voltage and current (i.e. in flux weakening) for AC drives of various types. The performance of the direct-flux vector control relies on the accuracy of the flux estimation, as for any field oriented control. The knowledge of the motor magnetic model is critical for flux estimation when the operating at low speed. This paper addresses the effects of a limited knowledge of the motor model on the performance of the control at low speed, for an Interior Permanent Magnet motor drive. Experimental results are given.**

I. INTRODUCTION

The main goals of the control of Interior Permanent Magnet (IPM) motor drives are a fast, linear torque control and a reliable exploitation of the inverter current and voltage limits in flux weakening operation. Basically, each IPM motor is custom designed for the specific application and the magnetic and operating specifications are so widespread and differentiated that it is not possible to think of controlling an IPM motor drive at its best by the simple knowledge of the motor nameplate data. There is even no standard notation in terms of nameplate and minimum set of parameters to be provided when dealing with such motors.

The current vector control of IPM motor drives has been proposed throughout the last twenty five years [1]. All the different control techniques focused on obtaining the Maximum Torque per Ampere (MTPA) operation at low speed, and a constant power speed range by means of flux weakening at high speed [2]. Both goals were obtained using open loop control techniques employing look-up tables [2-3]. Such tables require the knowledge and the manipulation of the motor magnetic model and make the control very sensitive to parameter uncertainty and variation. A very simple and effective closed-loop algorithm was then proposed in [4], relying on an additional control loop for maximum voltage limitation, but not capable of coping with the Maximum Torque Per Voltage (MTPV) speed operating region. To fill this gap, more and more complicated versions of [4] have been adopted, resulting in a cumbersome mix of tables and regulation loops to be tuned [5], or simpler schemes still heavily relying on the model [6]. Both solutions appear too difficult implementation-wise in the perspective of industrial applications.

Direct Torque Control (DTC), first applied to induction motor drives, has been extended to IPM motor drives for its high dynamic response and the position sensorless implementation [7]. Another important advantage of the DTC is its very straightforward attitude to flux weakening operation. DTC schemes with constant switching frequency have been investigated for reducing the torque ripple and making the inverter losses more predictable [8]. However, the DTC has to cope with flux estimation at zero and low speed and requires model based tables for MTPA operation [9], while MTPV is even not addressed in the literature.

Direct-Flux Vector Control (DFVC) has been proposed for IPM motor drives, aiming to combine the good characteristics of the DTC regarding the direct stator flux control and of the vector control regarding the current regulation of the torque current component [10]. DFVC is a vector control strategy implemented in stator flux reference frame, where the two controlled components are the flux linkage amplitude and the quadrature current component. As for DTC, torque control is linear, the control accuracy relies on flux estimation and the implementation of the flux weakening is very straightforward. As for current control, the switching frequency is constant and the current amplitude is directly limited by saturating the set point of the quadrature current component. The MTPV region can be also exploited by limiting the estimated flux load angle with a simple closed loop [11].

Dealing with MTPA operation, the IPM motor control techniques based on current vector control [1-6] make use of particular combinations of the d,q current component references, in the rotor synchronous frame. The DFVC obtains the MTPA by setting a proper stator flux amplitude reference according to the torque requirement [11].

A proper MTPA flux reference curve, along with an accurate flux estimation are the key issues for the DFVC. The machine voltage model based on stator back emf integration is very reliable for flux estimation only above a minimum operating speed. At low speed, the machine current model (magnetic model) should be used instead. This poses many problems for machines that are highly non-linear due to saturation and many possible rotor structures with different magnetic characteristics. For this reason, best results are obtained when the magnetic model is identified experimentally, an operation that requires a proper test equipment and specific expertise. This may be considered a key limiting factor against the widespread application of IPM motor drives, that are very often segregated to those application where the motor is custom designed.

The aim of the paper is to evaluate the effects of a simplified motor magnetic model over the performance of DFVC, for reducing as long as possible the need of an

accurate, off-line stage of motor identification. In particular, it will be systematically shown how the torque factor of the drive at low speed is diminished when different model simplifications are applied. All the model simplifications lead to a worse performance, with respect to the fully identified situation. Still, some simplifications are better than others and this will be outlined in order to find a tradeoff between accuracy and identification simplicity. Sensored operation is only considered here, but the conclusions of the paper are of general validity and could apply also to motion sensorless control.

II. DIRECT FLUX VECTOR CONTROL

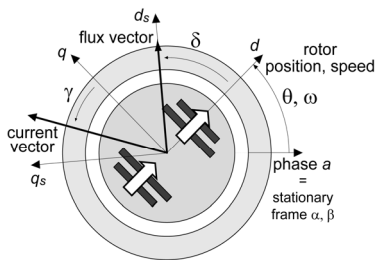

Fig. 1. Definition of the stator field oriented reference frame dq_s, the stationary frame αβ, the rotor frame dq, the current and flux vectors phase angles γ and load angle δ.

The reference axes, the rotor position and speed and the current and flux phase angles are defined in Fig. 1. The control scheme is described in [10-11] and it is based on the direct control of the flux linkage amplitude and the quadrature current component in the stator flux reference frame (d_s,q_s). The DFVC is based on (1,2):

$$\bar{v}_{dqs} = R_s \cdot \bar{i}_{dqs} + \frac{d}{dt} \cdot \begin{bmatrix} \lambda \\ 0 \end{bmatrix} + \lambda \cdot \begin{bmatrix} 0 \\ \omega + \frac{d\delta}{dt} \end{bmatrix} \quad (1)$$

$$T = \frac{3}{2} \cdot p \cdot \lambda \cdot i_{qs} \quad (2)$$

The flux amplitude λ is regulated with a proportional-integral (PI) flux controller whose output is the v_{ds} voltage component. The motor torque is regulated via the closed loop control of the quadrature current i_{qs} obtained with a PI controller whose output is the v_{qs} voltage component that will modify the motor load angle δ (Fig.1), according to the torque request.

The sensored, DFVC-based, speed control scheme of an IPM motor drive is reported in Fig. 2. The DFVC block regulates the stator flux and i_{qs} stator current and uses the measured rotor position, the measured currents and the estimated stator flux vector provided by the stator flux observer (FLUX OBS block in Fig.2).

Previous papers have shown that DFVC exhibits good performance in the flux-weakening speed range, i.e. for speed values higher that the base speed ω_b (end of the constant torque region) with a very limited impact of motor parameters [10,11]. On the contrary, the impact of the motor magnetic model on the low speed operation needs to be further analyzed. At this aim, the control blocks that are critical for low speed operation are considered in the following.

A. Stator flux observer

The stator flux observer (Fig.3) is a reduced-order, VIϑ closed-loop observer. The observer is based on the motor magnetic model (current-to-flux model) at low speed and on the motor voltage model (back-EMF integration) at high speed [10-12]. The magnetic model is represented in the (d,q) rotor frame defined in Fig. 1. The crossover angular frequency ω_{co} between low-speed and high speed models coincides with the observer gain g (rad/s), and it is usually much lower than the base speed ω_b. For speed values above the ω_{co} speed, the flux estimate is dominated by the voltage model that is extremely reliable, while for speed values below ω_{co} it depends of the accuracy of the magnetic model.

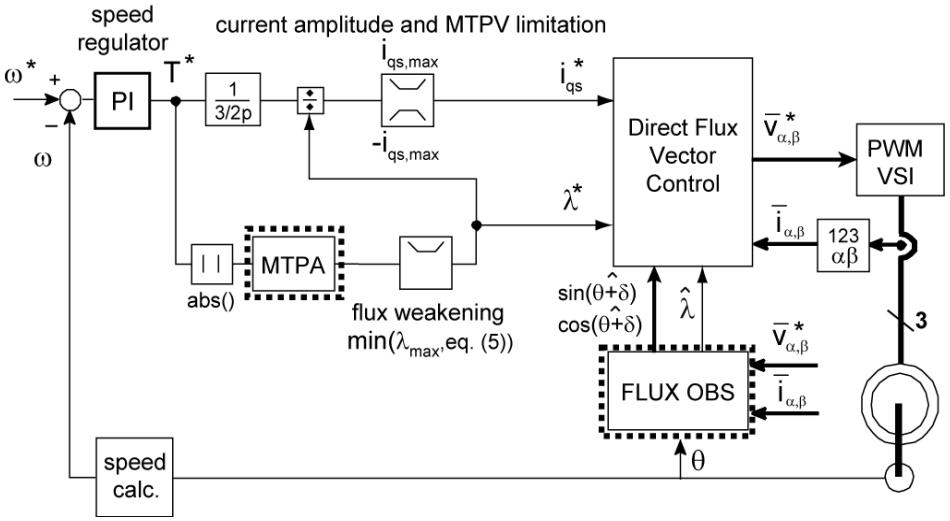

Fig. 2. Closed loop, sensored speed control scheme, based on direct flux vector control

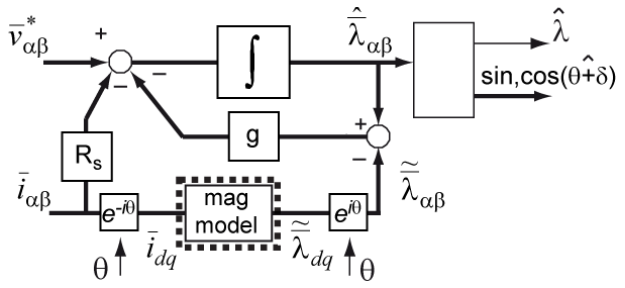

Fig. 3. Closed loop, reduced order flux observer.

The inaccuracies of the motor magnetic model produce amplitude and orientation errors of the flux estimate. In either cases (orientation or amplitude error), a discrepancy between the torque set point and the obtained electromagnetic torque arises. The paper is focused only on motor operation at speed values below the observer crossover speed ω_{co}.

B. MTPA block

The MTPA block (Fig. 2) is based on a look-up table, that associates the torque request to the flux amplitude reference that is proper for the maximum torque per Ampere ratio. Such control table requires the accurate knowledge of the motor model. Any error in the motor identification or any model simplification will lead to a non optimal torque versus Ampere ratio, at least in the constant torque speed region, that is below the base speed ω_b.

III. IPM MAGNETIC MODEL IN ROTOR FRAME

The IPM motor under test is a prototype designed for home appliances, rated 1.4 Nm continuous torque at low speed and 500W continuous power at 16000 rpm. The continuous current is 2.8 Apk while the peak overload current is 5Apk. The stator has 24 slots with overlapping windings. The rotor (Fig.4) is a 2-pole-pairs multilayer rotor, with plastic bonded ferrite magnets injected into the flux barriers. Motors of this type are also indicated as PM-assisted synchronous reluctance motors, characterized by a high saliency and a low per-unit value of the PM flux (…).

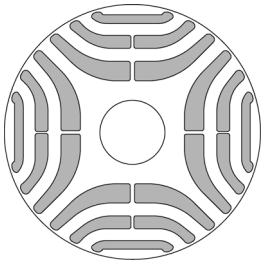

Fig. 4. Sketch of the IPM motor rotor. It is a 3-layer rotor with the injected plastic magnets.

C. Steady-state identification of the magnetic model

The identification of the motor requires a dedicated rig, time and expertise. The identification procedure needs a vector current control scheme implemented in rotor frame that imposes to the machine a set of a proper sequence of current pulses encompassing all possible motor current values in (d,q) frame, while the motor is rotated at constant speed by a speed controlled servomotor. Other details regarding this identification procedure are given in [13].

The motor has been thoroughly identified at steady-state within the range [-5,0] (Apk) for the d-axis and [0,5] (Apk) for the q-axis, including all the mutual combinations of the two current components. The flux versus current experimental characteristics are reported in Fig. 5. These flux characteristics will be the baseline of comparison with different simplified models. The no-load λ_d flux (PM flux linkage) is 0.06 Vs, while the λ_q flux has its saturation knee around 0.25 Vs. The effect of magnetic saturation is very evident in Fig. 5 along the q-axis, but in both subfigures the presence of multiple lines stands for cross-saturation, that is the mutual effect of a current component over the other axis flux component and is again a consequence of core saturation. In other words, the magnetic model is non linear and non diagonal as in (3):

$$\bar{\lambda}_{dq} = \begin{bmatrix} L_d(i_d, i_q) & -L_{dq}(i_d, i_q) \\ -L_{dq}(i_d, i_q) & L_q(i_d, i_q) \end{bmatrix} \cdot \bar{i}_{dq} + \begin{bmatrix} \lambda_m \\ 0 \end{bmatrix} \qquad (3)$$

where all the direct, quadrature and cross inductances are a function of i_d and i_q. The no-load flux linkage λ_m is variable according to the PMs temperature, but this effect is not considered in this work.

A. Simplified magnetic model

A simplified magnetic model such as (4) will be tested in the two different conditions indicated as “simpl 1” and “simpl 2” in Fig. 5 for implementation into the flux observer.

$$\bar{\lambda}_{dq} = \begin{bmatrix} L_d & 0 \\ 0 & L_q \end{bmatrix} \cdot \bar{i}_{dq} + \begin{bmatrix} \lambda_m \\ 0 \end{bmatrix} \qquad (4)$$

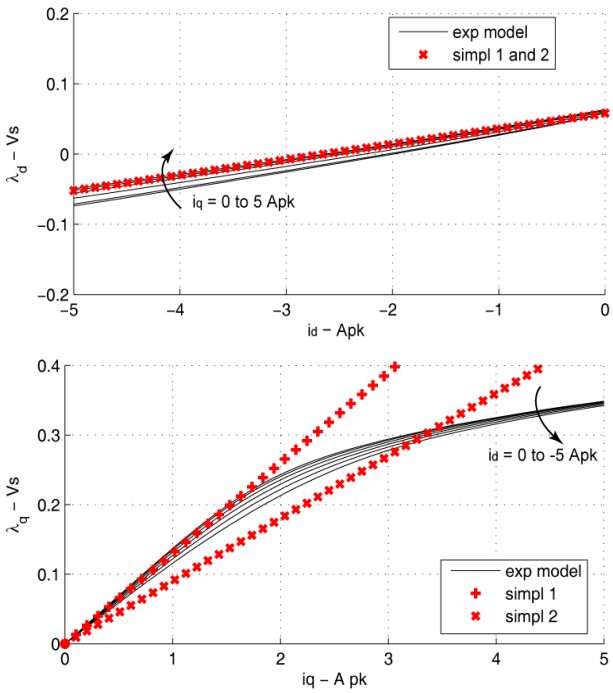

Fig. 5. Continuous lines: flux linkage characteristics of the IPM motor under test, measured at steady state and represented in the rotor synchronous frame (d,q). Cross-dotted lines: different model simplifications that will be tested in the following.

The model parameters in the two cases are reported in Table I. The model (4) will be used for flux estimation instead of the motor model tables but not for deriving the MTPA law.

Table I – Parameters of the linearized motor model in the two example tests.

	λ_m (Vs)	L_d (mH)	L_q (mH)
Simpl 1	0.06	22	130
Simpl 2	0.06	22	90

B. *Control trajectories and torque factor k_t*

The magnetic model shown in Fig.5 allows obtaining the motor control trajectories (MTPA, MTPV) shown in the (i_d,i_q) plane in Fig.6 along with the maximum current locus. The round marker at the corner between the MTPA and the 5 Apk circular trajectory is indicated with T_{max} and represents the maximum torque that is feasible with the maximum current amplitude.

The torque factor k_t (Nm/Apk) along the MTPA is also evaluated from the magnetic model and shown in Fig. 7. This torque factor is the best current to torque ratio that can be expected from the motor under test. Due to synchronous reluctance nature of the motor, k_t is low at low current values since part of the current has a magnetizing effect and not directly a torque effect and this is more evident at low loads.

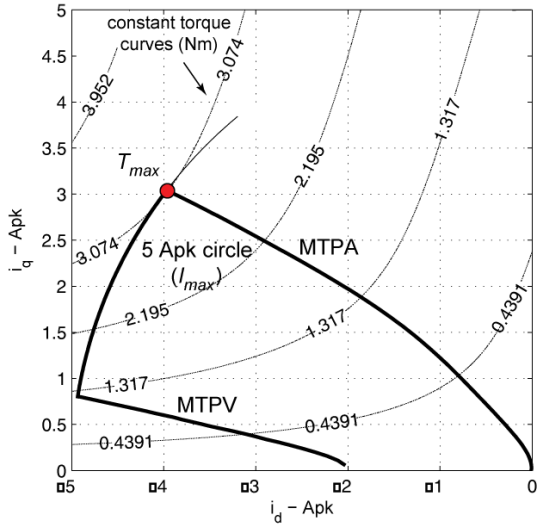

Fig. 6. Control trajectories calculated by manipulation of the experimental magnetic model of Fig. 5. The corner point between constant torque operation and flux weakening operation is put in evidence.

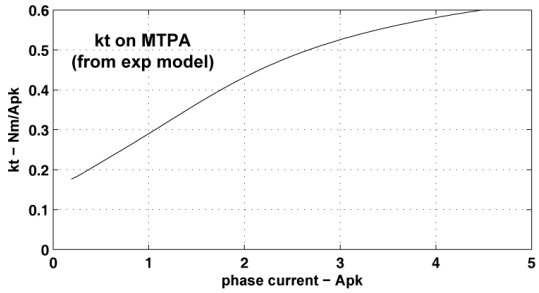

Fig. 7. Maximum torque factor k_t (Nm/Apk) of the IPM motor under test as a function of the current amplitude, calculated by manipulation of the experimental magnetic model of Fig. 5.

C. *Test of a simplified torque to flux reference law*

The torque to flux amplitude relationship along the MTPA, obtained from the experimental model, is reported in Fig. 8 along with three linear approximations. All the four control laws will be tested in control implementation and compared, within the "MTPA table" block in Fig. 2. The linear approximations are described as:

$$\lambda^* = \lambda_m + \frac{\lambda_1 - \lambda_m}{T_{max}} \cdot \left| T^* \right| \qquad (5)$$

where the PM flux linkage is applied at no load and the value λ_1 is applied with the maximum torque set point.

Three different λ_1 figures will be considered, equal, greater and lower than the correct value given by the MTPA table and called λ_{max} in the figure and in (5). All three laws have the correct no load flux value because it is assumed that the PM flux linkage is easily known from the motor nameplate or from the measurement of the back-EMF at no load.

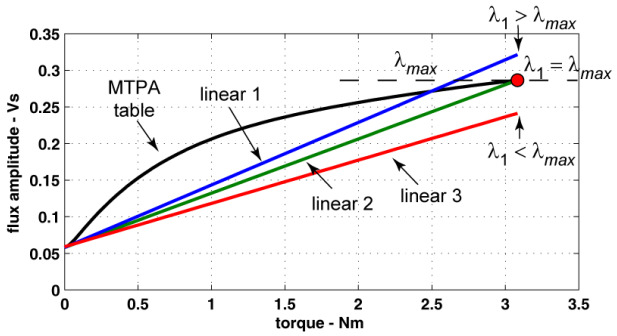

Fig. 8. Flux amplitude reference calculated by manipulation of the experimental magnetic model of Fig. 5 and linear simplifications that will be tested in the following.

IV. EXPERIMENTAL RESULTS

The IPM motor is fed by a 10 kHz IGBT inverter controlled by a dSPACE DS1103 board. The control sampling frequency is 10 kHz and uses the measured phase currents, the inverter DC link voltage and the rotor position. The rotor position is measured using a standard incremental encoder with 512 pulses per revolution. The inverter is fed by a single-phase rectifier supplied by 220V, 50Hz AC mains. The IPM motor is loaded with a current controlled DC motor fed by an industrial drive.

The IPM motor drive is speed controlled at 50 rpm, corresponding to a motor frequency of 1.67 Hz, which is well below the observer crossover frequency set at 40 Hz. The IPM motor is loaded progressively from zero to 2.5 Nm with the current controlled DC motor. The rise time of the load is 10 s from zero to 2.5 Nm for obtaining slowly variable steady state loading conditions. The same test is repeated 10 times with different implementations of the MTPA block of Fig. 2 and observer magnetic model block of Fig. 3, as described in the next subsections. For all tests, the trajectory of the stator current vector in the *(d,q)* plane and the torque factor k_t are presented and discussed.

A. *Effect of different MTPA laws when the flux is estimated correctly*

The flux observer employs the accurate magnetic model of Fig. 5, while the MTPA block implements all the four torque to flux laws shown in Fig. 8.

The trajectory of the stator current vector in the *(d,q)* plane for all tests and the torque factor k_t are illustrated in Fig. 10. With the MTPA table, the current trajectory follows the MTPA curve exactly (Fig. 10 top), despite the current vector is not controlled directly, and the k_t reproduces the calculated one (Fig. 10 bottom). The three linear simplifications of the MTPA control law deviate the current trajectories from the correct one and reduce, as expected, the k_t.

"Linear 3" gives the worse performance: the flux reference is under the correct value in all the torque range and the control compensates the low flux amplitude with a higher current. In turn, the maximum current limit is reached well below the maximum torque value T_{max}. "Linear 2" still gives lower flux values in all the torque range except for the maximum torque. In this case, the maximum torque can be obtained but with a k_t that is lower than expected. "Linear 1" gives the best performance: the k_t is lower than optimal in the range 0 to 3.5 Apk (that is 2.2 Nm) and then it is practically the correct one. In turn, ***it is better to overestimate the maximum flux reference with respect to λ_{max} than vice-versa.***

B. *Flux estimation from linear motor model "simpl 1"*

The flux observer employs the linear magnetic model "simpl 1" of Fig. 5; this model refers to the unsaturated value of the *q*-axis inductance.

The three linear control laws are compared in Fig. 11 showing a very poor performance in all three cases. In particular, the sudden deviation of the "linear 1" trajectory is due to the flux saturation to λ_{max} by the flux weakening block. In turn: ***the unsaturated, i.e. overestimated q-axis inductance value leads to overestimate the flux amplitude***. In this case, the "linear 1" is well above the performance of Fig. 10 due to the premature trigger of the flux saturation block. Consequently, the maximum torque is limited in all three cases.

C. *Flux estimation from linear motor model 2*

The flux observer employs the linear magnetic model "simpl 2" of Fig. 5, that refers to the saturated value of the *q*-axis inductance. The three linear control laws are compared in Fig. 12 showing that in this case "linear 1" is not far from the correct k_t at least for the high load region. In turn, ***the choice of the L_q term is critical and a proper choice can lead to a decent performance even with the very simple model (7) and a very simple flux reference law (linear 1)***.

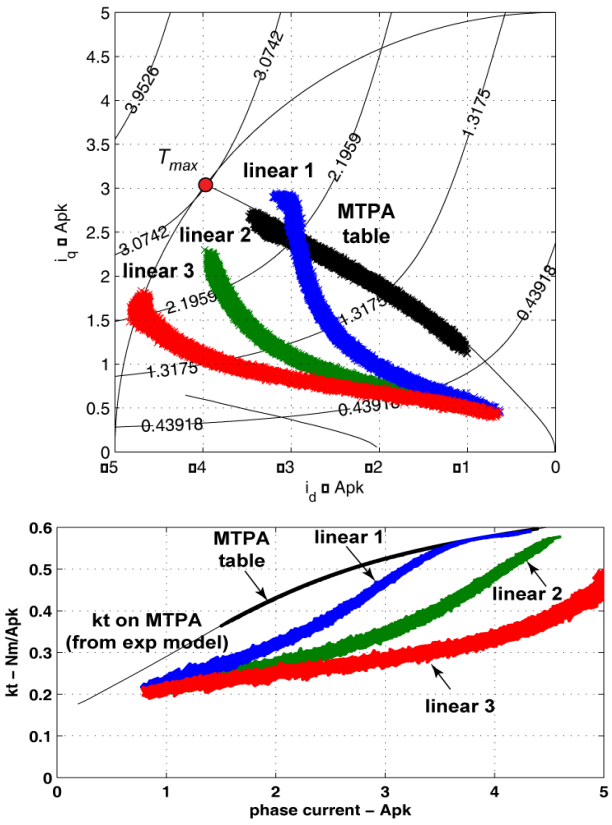

Fig. 10. Test at 50 rpm and variable load. The low speed flux mode is correct, four different torque to flux reference laws are compared. Top: Current trajectories; Bottom: torque to current ratio.

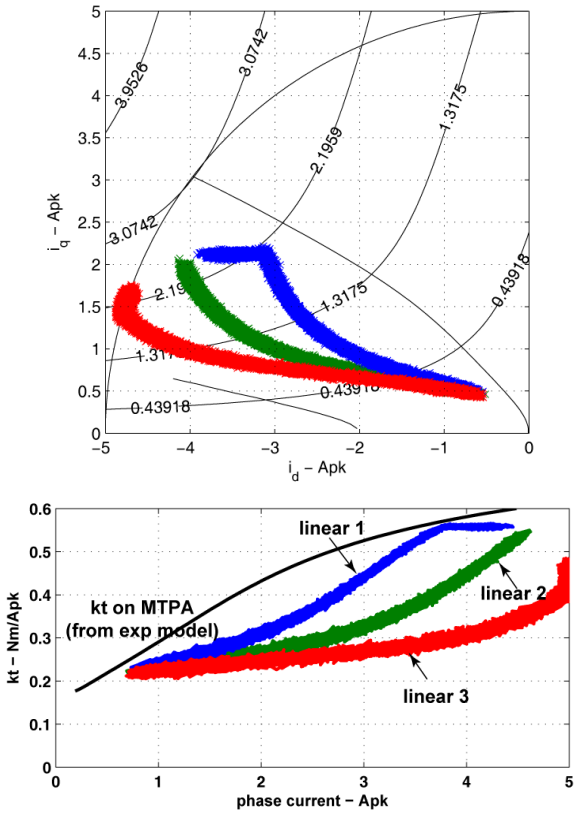

Fig. 11. Test at 50 rpm and variable load. The low speed flux model is the "linear 1" of Fig. 5. Three different torque to flux reference laws are compared. a) Current trajectories; b) torque to current ratio.

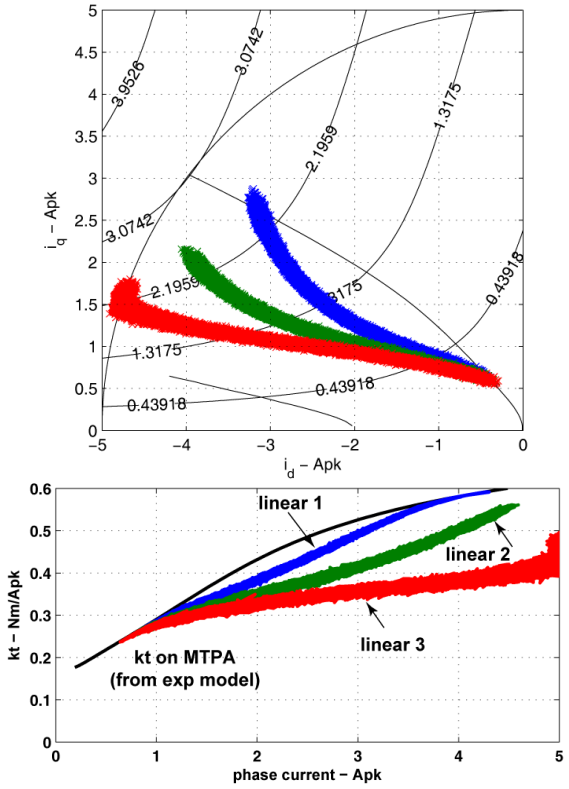

Fig. 12. Test at 50 rpm and variable load. The low speed flux model is the "linear 2" of Fig. 5. Three different torque to flux reference laws are compared. a) Current trajectories; b) torque to current ratio.

V. Conclusion

When compared with the correct MTPA table, simplified torque to flux laws lead to a non optimal exploitation of the motor. The torque factor k_t is lowered, meaning higher Joule losses. Still, if the simplified law is designed properly (e.g. linear 1 and 2) the linear control law is still capable of exploiting the full torque from the drive (T_{max}), even if the Joule losses are not minimized at partial loads.

At the same time, wrong choices (in particular linear 3) lead not only to higher motor losses, but also to a limited torque range, as shown in Fig.12 (bottom).

Improper values of L_q can make a very big difference. In particular, an unsaturated value of L_q leads to overestimate the flux and the torque is cut by premature flux weakening. On the contrary, an underestimate L_q would over saturate the motor incurring in a premature current limitation. The proper L_q should be chosen according to the maximum torque, maximum current condition: T_{max}, I_{max} on the MTPA.

The two critical values to be defined correctly are L_q and the flux saturation level $\lambda_{max,}$ that refer to the same working condition (T_{max}, I_{max} on the MTPA).

If the torque factor is critical at all load levels, then it is mandatory that the motor magnetic model is identified properly and the MTPA law must be computed from this model. The motor identification must be performed for all the current operating range.

Simplified control schemes may use linear magnetic models and MTPA laws, but that would reduce the torque factor. In any case, it is critical that the T_{max}, I_{max} condition is identified at least to determine the maximum flux linkage λ_{max} and the saturated L_q.

The paper used for the experimental tests an IPM prototype with 3-layer rotor and having a high reluctance torque component. For this reason, the results obtained in this paper can be considered valid for IPM machines with high anisotropy. Future work will focus also on IPM machines with high per-unit PM flux linkage.

References

[1] Jahns, Thomas M.; Kliman, Gerald B.; Neumann, Thomas W.; , "Interior Permanent-Magnet Synchronous Motors for Adjustable-Speed Drives," *Industry Applications, IEEE Transactions on* , vol.IA-22, no.4, pp.738-747, July 1986

[2] Jahns, Thomas M.; , "Flux-Weakening Regime Operation of an Interior Permanent-Magnet Synchronous Motor Drive," *Industry Applications, IEEE Transactions on* , vol.IA-23, no.4, pp.681-689, July 1987

[3] Morimoto, S.; Takeda, Y.; Hirasa, T.; Taniguchi, K.; , "Expansion of operating limits for permanent magnet motor by current vector control considering inverter capacity," *Industry Applications, IEEE Transactions on* , vol.26, no.5, pp.866-871, Sep/Oct 1990

[4] Jang-Mok Kim; Seung-Ki Sul; , "Speed control of interior permanent magnet synchronous motor drive for the flux weakening operation," *Industry Applications, IEEE Transactions on* , vol.33, no.1, pp.43-48, Jan/Feb 1997

[5] Bon-Ho Bae; Patel, N.; Schulz, S.; Seung-Ki Sul; , "New field weakening technique for high saliency interior permanent magnet motor," *Industry Applications Conference, 2003. 38th IAS Annual Meeting. Conference Record of the* , vol.2, no., pp. 898- 905 vol.2, 12-16 Oct. 2003

[6] Young-Doo Yoon; Wook-Jin Lee; Seung-Ki Sul; , "New flux weakening control for high saliency interior permanent magnet synchronous machine without any tables," *Power Electronics and Applications, 2007 European Conference on* , vol., no., pp.1-7, 2-5 Sept. 2007

[7] Rahman, M.F.; Zhong, L.; Khiang Wee Lim; , "A direct torque-controlled interior permanent magnet synchronous motor drive incorporating field weakening," *Industry Applications, IEEE Transactions on* , vol.34, no.6, pp.1246-1253, Nov/Dec 1998

[8] Swierczynski, D.; Kazmierkowski, M.P.; Blaabjerg, F.; , "DSP based direct torque control of permanent magnet synchronous motor (PMSM) using space vector modulation (DTC-SVM)," *Industrial Electronics, 2002. ISIE 2002. Proceedings of the 2002 IEEE International Symposium on* , vol.3, no., pp. 723- 727 vol.3, 2002

[9] Lixin Tang; Limin Zhong; Rahman, M.F.; Hu, Y.; , "A novel direct torque controlled interior permanent magnet synchronous machine drive with low ripple in flux and torque and fixed switching frequency," *Power Electronics, IEEE Transactions on* , vol.19, no.2, pp. 346- 354, March 2004

[10] Pellegrino, G.; Armando, E.; Guglielmi, P.; , "Direct Flux Field-Oriented Control of IPM Drives With Variable DC Link in the Field-Weakening Region," *Industry Applications, IEEE Transactions on* , vol.45, no.5, pp.1619-1627, Sept.-oct. 2009

[11] Pellegrino, G.; Bojoi, R.; Guglielmi, P.; , "Unified Direct-Flux Vector Control for AC motor drives," *Energy Conversion Congress and Exposition (ECCE), 2010 IEEE* , vol., no., pp.1150-1157, 12-16 Sept. 2010

[12] Anno Yoo; Seung-Ki Sul; , "Design of Flux Observer Robust to Interior Permanent-Magnet Synchronous Motor Flux Variation," Industry Applications, IEEE Transactions on , vol.45, no.5, pp.1670-1677, Sept.-Oct. 2009

[13] A. Vagati, M. Pastorelli, F. Scapino and G. Franceschini, "Impact of Cross Saturation in Synchronous Reluctance Motors of the Transverse-Laminated Type", IEEE Trans. Ind. Appl., Vol.36, No.4, July/August 2000, pp. 1039-1046.